MODELING AND DYNAMIC ANALYSIS OF ATOMIC FORCE MICROSCOPE BASED ON EULER-BERNOULLI BEAM THEORY

A. FARROKH PAYAM*, M. FATHIPOUR
Device Modeling and Simulation Lab, School of Electrical & Computer Engineering,University of Tehran, Tehran, Iran

Operation of atomic force microscope in dynamic mode has received great attention due to its ability to image compliant materials and also due to the fact that it can prevent the tip and sample damages during scanning. In this paper a model is proposed for AFM micro-cantilever-tip system based on Euler-Bernoulli beam theory and is solved numerically in order to study the behavior of a continuous cantilever beam in dynamic mode subject to changes in tip mass, cantilever density, length and the interaction force between the cantilever-tip and the sample. This is accomplished by linearizing the surface coupling force.

(Received September 1, 2009; accepted September 30, 2009)

Keywords: Modeling, Atomic force Microscopy, Euler-Bernoulli theory

1. Introduction

Atomic force microscope (AFM) is a powerful tool for imaging, manipulation and lithography in nanometer. After its invention in 1986 by Binning *et al.* [1] several improvements have been made [2]. In particular, AFM has been utilized in dynamic mode for imaging and manipulation [3]. The atomic force microscope utilizes a sharp tip which moves over the surface of the sample in a raster scan mode to measure the topography and material properties of the surface. The tip is located at the free end of a cantilever micro beam (probe) which may bend in response to the interaction forces between the tip and the sample. An estimate of the micro beam stiffness may be used to determine the interaction forces from measurements of these deflections.

To understand properties and characteristics of this mode of operation, complete dynamic analysis of atomic force microscope is necessary [3-7]. Modeling of micro-cantilever-tip system and the interaction between tip and sample play an important role in the study of AFM dynamic operation. The dynamic response of the AFM cantilever has been investigated by many researchers. There are two different modeling approaches for AFM cantilever-tip system and its dynamics [8]. Lumped parameter modeling [9-12] and distributed parameter modeling [13-19]. In lumped parameter modeling, cantilever is approximated by a single degree of freedom harmonic oscillator is called first mode approximation [10-12]. Using this approximation, the equation of AFM cantilever motion is solved by ordinary differential equations. Various models have been proposed to analyze the dynamic behavior of AFM using this approach. However, in this approach, infinite numbers of resonant frequencies of cantilever-tip system are neglected. The distributed nature of structural flexibility in the AFM cantilever has direct influence on the image resolution and is preferred for modeling AFM cantilever.

Distributed parameter modeling provides greater insight into the fundamental characteristics of the AFM dynamics. The micromechanical AFM cantilever in a distributed parameter model is considered as a multiple degrees of freedom (MDOF) system allowing for consideration of higher resonance frequencies in AFM [13–20]. In [13] the cantilever dynamics was modeled as a linear time-invariant system with a nonlinear output feedback to incorporate the tip-sample interaction. However, the tip-mass and the excitation of cantilever support were neglected in the AFM model. Transfer function of the AFM micro cantilever is analyzed in [14]-[15]. Several other distributed models based on Euler-Bernoulli beam theory are suggested in [16]-[19]. All of these methods are based on classical Euler-Bernoulli beam model and neglect rotary inertia, shear deformation, axial effects and the tip mass. In addition, study the effects of interaction forces on the resonance frequencies and frequency response of the cantilever has not been carried out in most of them.

In this paper, to study the effect of cantilever tip mass, tip-surface interacting forces, cantilever length and density on the system dynamics and resonance frequencies, using Euler-Bernoulli model and Hamilton principle [21]-[24] a comprehensive model for AFM micro cantilever system is developed.

In section 2, we provide a distributed parameter model for the AFM micro cantilever-tip based on Euler-Bernoulli method which takes into account the effect of tip mass. In section 3, the governing equations of motion are solved analytically. In section 4, the results obtained are analyzed using a numerical case study and the effects of tip mass, cantilever length, density and linearized interaction force (tip-sample stiffness) on the system dynamics are investigated and analyzed. Finally a conclusion is presented.

2. Modeling

To obtain the dynamic equation of the AFM micro cantilever system, we use Euler-Bernoulli beam theory. Detailed derivations for the Euler-Bernoulli model can be found in text books [22]-[24]. Fig.1 shows a schematic of distributed parameter model for the AFM system.

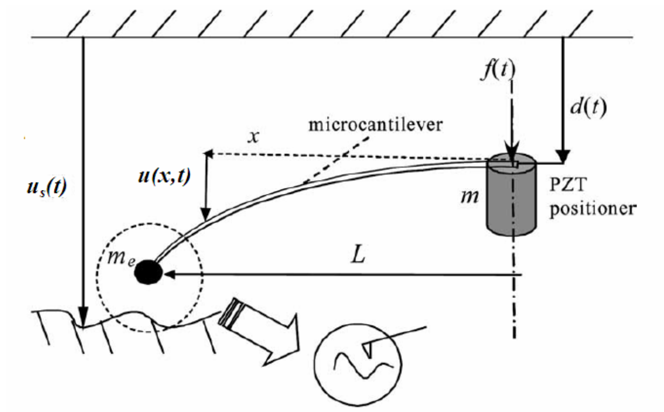

Fig. 1. Schematic of distributed parameter model of the AFM system [16].

To derive the equation of motion we assume that:

1- The AFM micro-cantilever is modeled as a flexible cantilevered beam with an equal cross section and density.

2- The effect of shear deformation is neglected.

3- Speed of motion for the platform is assumed negligible.

4- There is no relative motion between the cantilever head end and the platform.

5- One end of the cantilever beam is clamped to the base position with the mass m, while the tip mass m_e is attached to the free end of the micro-cantilever beam, as depicted in Fig.1.

6- The rigidity of the beam is EI, its length and density are L and ρ respectively.

In this modeling we also consider the viscous air damping and structural damping for the micro-cantilever motion [16]. The equation of motion is obtained using Hamilton's variation principle. The potential energy of a uniform beam due to bending is given by

$$PE = \frac{1}{2}\int_0^L EIu_{xx}^2(x,t)dx \tag{1}$$

Where $u(x,t) \in \Re^1$ is the lateral displacement of the micro-cantilever beam with respect to its base. And the subscript $()_x$ indicates the partial derivative with respect to position variable.

The kinetic energy is given by:

$$KE = \frac{1}{2}\dot{d}^2(t) + \frac{1}{2}m_e(\dot{d}(t) + u_t(L,t))^2 + \frac{1}{2}\int_0^L \rho(\dot{d}(t) + u_t(x,t))^2 dx \quad (2)$$

Where $d(t), \dot{d}(t), \ddot{d}(t)$ are the unit displacement (i.e. the PZT positioner), velocity and acceleration, respectively. And the subscript $()_t$ indicates the partial derivative with respect to the time variable.
Hamilton's principle may be stated as:

$$\int_{t_1}^{t_2} (\delta T - \delta U + \delta W_{nc})dt = 0 \quad (3)$$

Where T is the kinetic energy, U is the potential energy of the system, $\delta()$ is the first variation in the quantity in the parentheses and δW_{nc} is the work done by the nonconservative forces. t_1, t_2 are two arbitrary times at which the configuration of the system is known.
In this system, the virtual work due to the non-conservative transverse force is:

$$\delta W_{nc} = f(t)\delta d + f_{ID}(t)\delta u(L,t) - B\int_0^L u_t(x,t)dx\delta u(x,t) - C\int_0^L u_{xx}(x,t)dx\delta u(x,t) \quad (4)$$

Where B and C are the viscous and structural damping coefficients, respectively. $f(t)$ is the input control force and $f_{ID}(t)$ is the atomic interaction force given by:

$$f_{ID}(t) = \begin{cases} -\dfrac{HR}{6(u_s - u(L,t))^2} & z_s - u(L,t) \geq a_0 \\ -\dfrac{HR}{6a_0^2} + \dfrac{4}{3}E^*\sqrt{R}(u_s - u(L,t) + a_0)^{3/2} & z_s - u(L,t) < a_0 \end{cases} \quad (5)$$

Note that this equation governs the interaction force in the repulsive regime according to a Derjaguin-Mu¨ller-Toporov (DMT model). H is hamacker constant, u_s is distance between the fixed base frame coordinate to the sample. R is the tip radius and parameter a_0 is the interatomic distance [13]. E^* is the effective elastic modulus calculated by:

$$E^* = \left[\frac{(1 - {v_t}^2)}{E_t} + \frac{(1 - {v_s}^2)}{E_s}\right]^{-1} \quad (6)$$

where E_t and E_s are the respective elastic moduli and v_t and v_s are the Poisson ratios of the tip and the sample, respectively.
Substituting equations (1), (2) and (4) in (3), the governing equations for micro cantilever can be obtained as:

$$\begin{aligned} &\rho(u_{tt}(x,t) + \ddot{d}(t)) + Bu_t(x,t) + Cu_{tt}(x,t) + EIu_{xxxx}(x,t) = 0 \\ &(m + \rho L + m_e)\ddot{d}(t) + \int_0^L \rho u_{tt}(x,t)dx + m_e u_{tt}(L,t) = f(t) + f_{ID}(t) \end{aligned} \quad (7)$$

With the boundary conditions:

$$\begin{aligned} &m_e(\ddot{d}(t) + u_{tt}(L,t)) - EIu_{xxx}(L,t) = f_{ID}(t) \\ &u(0,t) = u_x(0,t) = u_{xx}(L,t) = 0 \end{aligned} \quad (8)$$

The boundary conditions provided by van der Waalse and DMT tip-sample forces model which are nonlinear. They are linearized using a binomial expansion. In this case, we consider that the

system stays in a small enough neighborhood of the equilibrium set point u_0, which can be adjusted moving the sample relative to the cantilever mount [14], [18].
By linearizing the interaction force around z_0 we have:

$$f_{ID} = -k_{ts} u(L,t) \tag{9}$$

Where the contact stiffness, k_{ts} is given by:

$$k_{ts} = -\frac{\partial f_{ID}(t)}{\partial u(L,t)}\Big|_{u=u_0} \tag{10}$$

Considering equations (5) and (10), we have:

$$k_{ts} = \begin{cases} -\dfrac{HR}{3(z_s - z_0)^3} & z_s - z_0 \geq a_0 \\ 2E^* \sqrt{R}(a_0 + z_s - z_0)^{1/2} & z_s - z_0 < a_0 \end{cases} \tag{11}$$

Note that the sign of k_{ts} depends on the regime of the interaction force. It is negative when the force is attractive and positive when the force is repulsive [14].
Considering:

$$k_{ts} = \frac{3EI}{L^3} \hat{k}_{ts} \tag{12}$$

$\hat{k}_{ts}$ is a parameter which determines the magnitude and regime of interaction force and $k = 3EI / L^3$ is the cantilever spring constant.

3. Solution of Governing Equation

The equation of motion, boundary conditions, and initial conditions form an initial-boundary-value problem which can be solved for example by using separation of variables and eigenfunction expansion.

If sinusoidal vibrations of the cantilever base are assumed to excite the system by an amplitude D and angular frequency ω this signal is selected:

$$d(t) = D \sin \omega t \tag{13}$$

We assume the structural and viscous dampings are neglected. Therefore the governing equation converted to:

$$EIu_{xxxx}(x,t) + \rho u_{tt}(x,t) = -\rho \ddot{d}(t) \tag{14}$$

Using the method of separation of variable, we write:

$$u(x,t) = W(x)T(t) \tag{15}$$

Substituting (13) and (15) in (14), we have:

$$\begin{gathered} \ddot{T}(t) + \omega^2 T(t) = 0 \\ W^{(4)}(x) - a^4 W(x) = a^4 D \end{gathered} \tag{16}$$

With the boundary conditions as:

$$\begin{gathered} -m_e \omega^2 (D + W(L)) - EIW'''(L) - F_{ID} = 0 \\ W(0) = W'(0) = W''(L) = 0 \end{gathered} \tag{17}$$

Where:

$$F_{ID} = -k_{ts} W(L) \tag{18}$$

And:

$$a^4 = \frac{\omega^2 \rho}{EI} \tag{19}$$

Equation (19) is called the dispersion relationship.
From Equations (16), $T(t)$ is sinusoidal in time, and $W(x)$ has both sinusoidal and hyperbolic terms:

$$\begin{aligned} T(t) &= T_1 \sin \omega t + T_2 \cos \omega t \\ W(x) &= W_h(x) + W_p(x) = C_1 \sin ax + C_2 \cos ax + C_3 \sinh ax + C_4 \cosh ax + W_p(x) \end{aligned} \tag{20}$$

Where T_i and C_i are constant coefficients.
From (17) we have four boundary conditions in terms of $W_h(x)$ only. They are applied to the spatial solution to obtain the corresponding frequency equations and eigenfunctions.
Substituting (16) in (20) gives eignfunction (modal shapes) as:

$$W_h(x) = \frac{m_e\omega^2[\cos aL + \cosh aL](\sin ax - \sinh ax) - m_e\omega^2[\sin aL + \sinh aL](\cos ax - \cosh ax)}{2[k_{ts} - m_e\omega^2][\sin aL \cosh aL - \cos aL \sinh aL] + 2a^3 EI[1 + \cos aL \cosh aL]} D \tag{21}$$

And the frequency characteristic equation is given by:

$$2[k_{ts} - m_e\omega^2][\sin aL \cosh aL - \cos aL \sinh aL] + 2a^3 EI[1 + \cos aL \cosh aL] = 0 \tag{22}$$

Details of calculation are given in the Appendix I.
The resonance frequencies are obtained as:

$$\omega_n = \sqrt{\frac{EI}{\rho}} a_n^2 \tag{23}$$

Where wave numbers a_n are calculated from (22).
The particular solution of the $W(x)$ from (16) is:

$$W_p(x) = -D \tag{24}$$

And the general solution of (16) is:

$$W(x) = \frac{m_e\omega^2[\cos aL + \cosh aL](\sin ax - \sinh ax) - m_e\omega^2[\sin aL + \sinh aL](\cos ax - \cosh ax)}{2[k_{ts} - m_e\omega^2][\sin aL \cosh aL - \cos aL \sinh aL] + 2a^3 EI[1 + \cos aL \cosh aL]} D - D \tag{25}$$

Due to consideration of interaction forces and tip mass this model is more comprehensive than those recently published for AFM micro cantilever system [15], [18] and [19].

4. Numerical Analysis and Case Study

To verify the accuracy of the presented model and to investigate the effects of tip mass, interaction forces, length and density of the micro-cantilever on the frequency response of the system, numerical analyses are carried out. Physical parameters accounted for the system are summarized in Table I.

Table 1. The physical parameters of the system.

PROPERTIES	SYMBOL	VALUE	UNIT
Beam Rigidity	EI	4.854e-13	Nm^2
Beam Thickness	t_b	4	μm
Beam Width	b	35	μm
Beam Length	L	500	μm
Tip Radius	R	5	nm
Intermolecular Distance	a_0	1.2	nm
AFM Base Motion Amplitude	D	7	nm
Beam Linear Density	ρ	3.262e-7	kg/m
Beam Mass of AFM	m	0.001	kg
AFM Tip Mass	m_e	3e-11	kg
Hamacker Constant	H	10e-19	J

The sensitivity of modes and resonance frequencies of an AFM cantilever is defined as the change in the flexural vibration frequency of a mode to the change in the tip-sample interaction. Hence, the oscillating cantilever is assumed to be in linear force interaction with a variety of vertical contact stiffness.

In the first test we calculate the resonance frequencies of the micro-cantilever where the tip mass and the linearized interaction force are ignored. In this case, the frequency characteristic equation is given by:

$$\left[1+\cos aL \cosh aL\right]=0 \tag{24}$$

And the normalized natural frequencies and wave numbers are given in Table II. Note that in this case the first natural frequency of the micro-cantilever beam is $1.7173\times10^4 (rad/\sec)$ which is the first resonance frequency of micro-cantilever if tip mass and interaction force is neglected.

Table 2. The characteristics of the system natural modes.

MODE	EIGNVALUE	NATURAL FREQUENCY
1	1.876	1
2	4.695	6.263
3	7.855	17.531
4	10.996	34.356
5	14.138	56.795
6	17.279	84.834
7	20.421	118.491
8	23.562	157.746
9	26.704	202.622
10	29.846	253.108
11	32.987	309.186
12	36.129	370.890

In the second test, we consider the effects of tip mass on the dynamics of AFM. For this purpose we consider three values for $\hat{k}_{ts} = -.1, 0, .1$. Figs. 2-4. Tables III-V show the normalized resonance frequencies obtained by numerical analysis in the attractive, free oscillating and repulsive regimes, respectively.

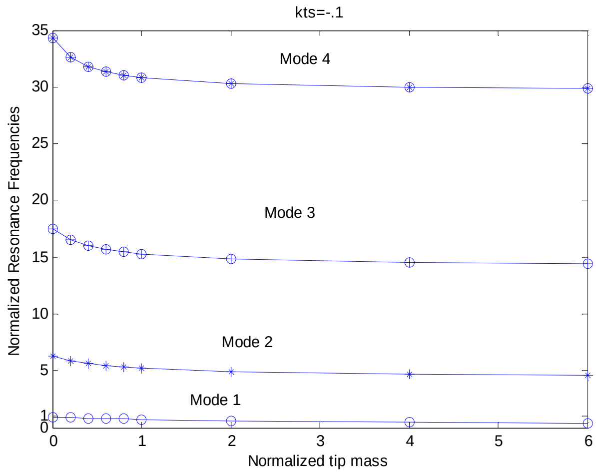

Fig.2. First four normalized resonance frequencies of the micro-cantilever as a function of normalized tip mass in the attractive regime.

Table 3. Normalized resonance frequencies of the micro-cantilever as a function of normalized tip mass in the attractive regime.

MODES\NORMALIZED MASS	0	.2	.4	.6	.8	1	2	4	6
1	0.949	0.886	0.833	0.789	0.751	0.718	0.599	0.473	0.403
2	6.255	5.882	5.631	5.450	5.317	5.212	4.912	4.690	4.598
3	17.531	16.580	16.037	15.693	15.454	15.282	14.836	14.549	14.440
4	34.355	32.652	31.822	31.343	31.033	30.820	30.296	29.985	29.869
5	56.793	54.212	53.118	52.530	52.167	51.921	51.354	51.018	50.904
6	84.831	81.276	79.955	79.279	78.881	78.607	78.012	77.664	77.552
7	118.488	113.880	112.349	111.605	111.177	110.896	110.269	109.922	109.799
8	157.741	152.036	150.319	149.523	149.080	148.781	148.131	147.781	147.664
9	202.616	195.740	193.880	193.050	192.576	192.266	191.601	191.247	191.129
10	253.101	245.042	243.043	242.163	241.666	241.351	240.689	240.325	240.209
11	309.177	299.912	297.792	296.873	296.378	296.047	295.369	295.003	294.893
12	370.880	360.361	358.1391	357.1915	356.688	356.365	355.661	355.300	355.179

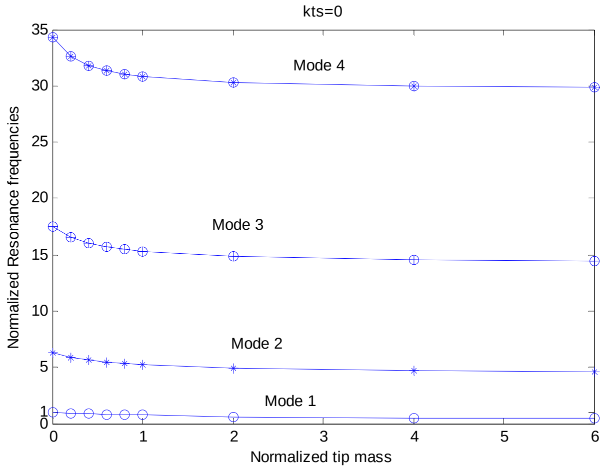

Fig.3. First four normalized resonance frequencies of the micro-cantilever as a function of normalized tip mass in the absent of interaction force.

Table 4. Normalized resonance frequencies of the micro-cantilever as a function of normalized tip mass in the attractive regime.

MODES\NORMALIZED MASS	0	.2	.4	.6	.8	1	2	4	6
1	1	0.932	0.878	0.831	0.791	0.756	0.632	0.499	0.425
2	6.263	5.890	5.636	5.455	5.319	5.214	4.912	4.690	4.598
3	17.531	16.580	16.037	15.693	15.454	15.282	14.836	14.549	14.440
4	34.355	32.652	31.822	31.343	31.033	30.820	30.296	29.985	29.869
5	56.793	54.212	53.118	52.530	52.167	51.921	51.354	51.018	50.904
6	84.831	81.276	79.955	79.279	78.881	78.607	78.012	77.664	77.552
7	118.488	113.880	112.349	111.605	111.177	110.896	110.269	109.922	109.799
8	157.741	152.036	150.319	149.523	149.080	148.781	148.131	147.781	147.664
9	202.616	195.740	193.880	193.050	192.576	192.266	191.601	191.247	191.129
10	253.101	245.042	243.043	242.163	241.666	241.351	240.689	240.325	240.209
11	309.177	299.912	297.792	296.873	296.378	296.047	295.369	295.003	294.893
12	370.880	360.361	358.139	357.191	356.688	356.365	355.661	355.300	355.179

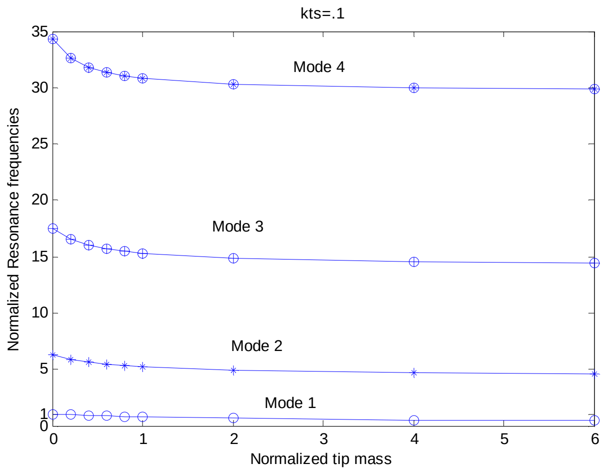

Fig.4. First four normalized resonance frequencies of the micro-cantilever as a function of normalized tip mass in the repulsive regime.

Table 5. Normalized resonance frequencies of the micro-cantilever as a function of normalized tip mass in the repulsive regime.

MODES\NORMALIZED MASS	0	.2	.4	.6	.8	1	2	4	6
1	1.046	0.977	0.919	0.871	0.829	0.793	0.663	0.523	0.446
2	6.268	5.895	5.641	5.458	5.322	5.217	4.914	4.690	4.598
3	17.535	16.584	16.037	15.693	15.454	15.282	14.836	14.549	14.440
4	34.355	32.658	31.822	31.343	31.033	30.820	30.296	29.985	29.869
5	56.793	54.212	53.118	52.530	52.167	51.921	51.354	51.018	50.904
6	84.831	81.276	79.955	79.279	78.881	78.607	78.012	77.664	77.552
7	118.488	113.880	112.349	111.605	111.177	110.896	110.269	109.922	109.799
8	157.741	152.036	150.319	149.536	149.080	148.781	148.131	147.781	147.664
9	202.616	195.740	193.880	193.050	192.576	192.266	191.601	191.247	191.129
10	253.101	245.042	243.043	242.163	241.666	241.351	240.689	240.325	240.209
11	309.177	299.912	297.792	296.873	296.378	296.047	295.369	295.003	294.893
12	370.880	360.361	358.139	357.191	356.688	356.365	355.661	355.300	355.179

As expected, from data in Figs.2-4 and Tables III-V, it can be seen that increasing of the tip mass decreases the resonance frequencies of the system. Also, the resonance frequencies of the system are increased in the repulsive regime and are decreased in the attractive regime of the interaction force.

In the third test, the effects of interaction forces on the AFM microcantilever dynamics are studied. The first resonance frequency in this test is: $1.2996\times10^{4}(rad/\sec)$ which is related to the free oscillating micro-cantilever system with its nominal tip mass. For $\hat{k}_{ts}<-1$ the snap-in event occurs [14] and therefore not considered here. Results shown in Table VI confirm the validity of the presented model and depict the fact that, an attractive interaction results in a shift to lower frequencies and in contrast, repulsive interactive results in a shift to higher frequencies.

Table 6. Normalized resonance frequencies of the micro-cantilever as a function of normalized linearized effective spring constant.

MODES\NORMALIZED EFFECTIVE SPRING CONSTANT	-.1	-.01	0	.1	1	10	100
1	0.949	0.995	1	1.048	1.407	3.140	5.467
2	6.887	6.890	6.890	6.893	6.9197	7.249	12.100
3	20.194	20.194	20.194	20.194	20.200	20.249	20.990
4	40.726	40.726	40.726	40.726	40.726	40.742	40.914
5	68.609	68.609	68.609	68.609	68.609	68.619	68.680
6	103.872	103.872	103.872	103.872	103.872	103.884	103.909
7	146.540	146.540	146.540	146.540	146.540	146.540	146.554
8	196.600	196.600	196.600	196.600	196.600	196.600	196.600
9	254.061	254.061	254.061	254.061	254.061	254.061	254.061
10	318.923	318.923	318.923	318.923	318.923	318.923	318.945
11	391.19	391.19	391.19	391.19	391.19	391.19	391.19

	9	9	9	9	9	9	9
12	470.90 4	470.90 4	470.90 4	470.90 4	470.90 4	470.90 4	470.90 4

To study the effects of cantilever length on resonance frequency, another numerical analysis is carried out and its results are given in Table VII. It is observed that increasing the cantilever length, decreases the resonance frequencies.

Table 7. Normalized resonance frequencies of the micro-cantilever as a function of normalized cantilever length

MODES\NORMALIZED CANTILEVER LENGTH	.2	.4	.6	.8	1	2	4	6	8	10
1	15.139	4.865	2.447	1.484	1	0.281	0.075	0.034	0.0197	0.012
2	153.124	39.909	18.301	10.551	6.890	1.829	0.480	0.218	0.124	0.080
3	478.513	121.647	54.834	31.219	20.194	5.234	1.356	0.613	0.348	0.224
4	988.274	249.240	111.635	63.232	40.726	10.425	2.675	1.205	0.684	0.440
5	1683.155	423.054	188.949	106.758	68.609	17.437	4.448	2	1.133	0.729
6	2563.502	643.126	286.801	161.832	103.872	26.284	6.675	2.996	1.696	1.090
7	3628.721	909.581	405.244	228.459	146.540	36.973	9.361	4.195	2.373	1.525
8	4879.416	1222.209	544.251	306.678	196.600	49.507	12.507	5.598	3.164	2.033
9	6315.455	1581.299	703.828	396.452	254.061	63.887	16.112	7.205	4.071	2.614
10	7937.013	1986.574	883.953	497.804	318.923	80.119	20.178	9.016	5.092	3.268
11	9743.059	2438.184	1084.713	610.719	391.199	98.200	24.706	11.032	6.228	3.997
12	11735.406	2936.175	1306.00	735.206	470.904	118.131	29.694	13.253	7.478	4.798

Finally the effects of cantilever density on the frequencies of the system are investigated and the results are shown in Figs. 5-7.

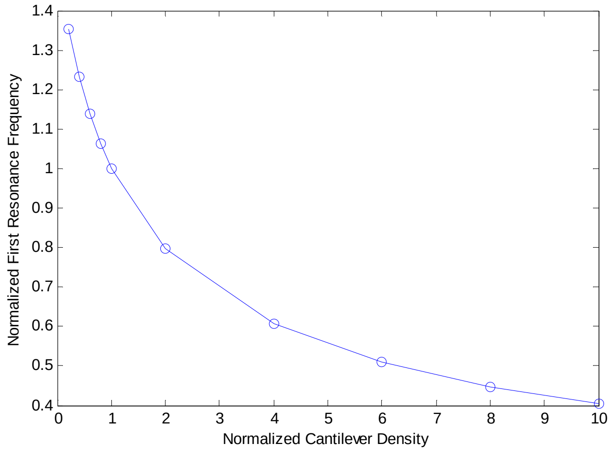

Fig.5. Effect of density of the tip on the first resonance frequency.

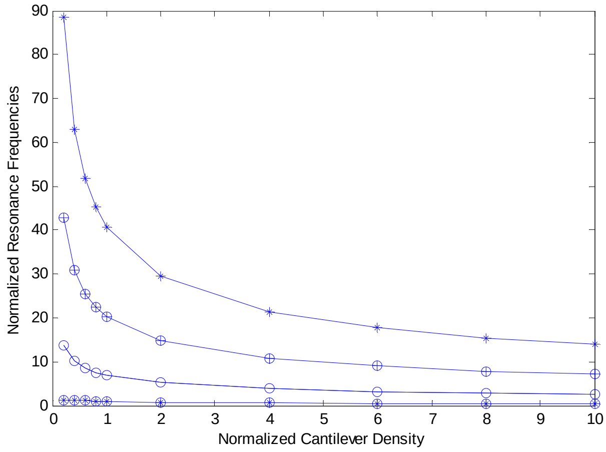

Fig.6. Effect of density of the tip on the first four resonance frequencies.

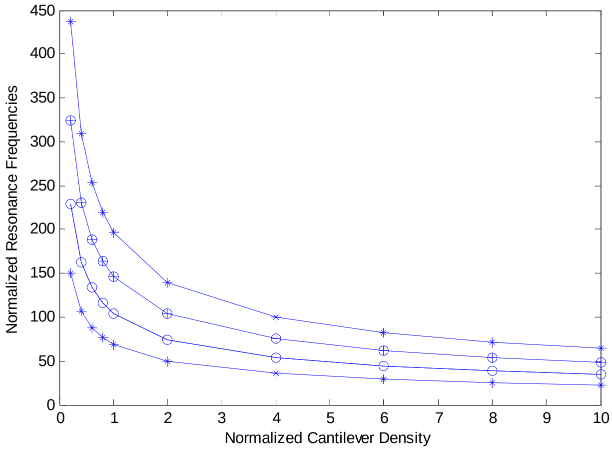

Fig.7. Effect of density of the tip on fifth to eighth resonance frequencies.

It is seen from these figures that the tip density has considerable influence on the resonance frequencies for modes in higher frequency regions. The resonance frequencies decrease as the tip density increase in all modes and this effect is more pronounced for higher order frequencies.

5. Conclusions

In this paper based on Euler-Bernoulli beam theory and by considering tip mass and linearized interaction force between cantilever-tip and sample, a distributed parameter model for AFM micro-cantilever-tip system is presented and using separation method the governing equation is solved analytically.

The effects of tip mass, attractive and repulsive interaction force, cantilever density and length on the resonance frequencies of the system are studied by numerical analysis. Increasing the tip mass decreases the resonance frequencies, especially in higher frequencies. There is a positive shift in resonance frequencies in the repulsive interaction region and a negative shift in the attractive regime. Also, the cantilever density and length affect the system frequencies. The major contribution of this paper is consideration of tip mass in the Euler-Bernolli distributed parameter model of the AFM and the study its effects on system resonance frequencies. It is concluded from this analysis that neglecting the tip mass has a considerable effect on the dynamic analysis of AFM especially in higher modes.

References

[1] G. Binnig, C. Gerber, and C. Quate, “Atomic force microscope”, Phys. Rev. Lett., vol. 56, pp. 930-933, 1986.

[2] Daniel Y. Abramovitch, Sean B. Andersson, Lucy Y. Pao, and Georg Schitter, A Tutorial on the Mechanisms, Dynamics, and Control of Atomic Force Microscopes, Proceedings of the 2007 American Control Conference Marriott Marquis Hotel at Times Square New York City, USA, July 11-13, 2007.

[3] Ricardo Garcia, Ruben Perez, Dynamic Atomic Force Microscopy Methods, Surface Science Methods 47 (2002), 197-301.

[4] U. Rabe, K. Janser and W. Arnold, “Vibrations of free and surfacecoupled atomic force microscope cantilevers: theory and experiment,” Review of Scientific Instruments, vol. 67, no. 9, pp. 3281–3293, 1996.

[5] S. Hirsekorn, “Transfer of mechanical vibrations from a sample to an AFM-cantilever— a theoretical description,” Applied Physics A, vol. 66, pp. S249–S254, 1998.

[6] D.W. Dareing, T. Thundat, J. Sangmin, M. Nicholson, “Modal analysis of microcantilever sensors with environmental damping,” Journal of Applied Physics, vol. 97, no. 8, 084902, 2005.

[7] D.R. Sahoo, A. Sebastian and M.V. Salapaka, “Transient-signal-based sample-detection in atomic force microscopy,” Applied Physics Letters, vol. 83, no. 26, pp. 5521–5523, 2003.

[8] N. Jalili and K. Laxminarayana, “A review of atomic force microscopy imaging systems: application to molecular metrology and biological sciences”, Mechatronics, vol. 14, pp. 907–945, 2004.

[9] Burnham NA, Behrend OP, Oulevey F, Gremaud G, Gallo PJ, Gourdon D, et al. How does a tip tap? Nanotechnology 1997;8(2):67–75.

[10] M. Ashhab, M. V. Salapaka, M. Dahleh, and I. Mezic, “Melnikov-Based Dynamical Analysis of Microcantilevers in Scanning Probe Microscopy,” Nonlinear Dynamics, vol. 20, pp. 197-220, 1999.

[11] Y. Fang, M. Feemster, D. Dawson, and N. M. Jalili, “Nonlinear control techniques for an atomic force microscope system”, Control Theory & Applications Journal, vol. 3, pp. 85-92, 2005.

[12] A. Sinha, “Nonlinear dynamics of atomic force microscope with PI feedback”, Journal of Sound and Vibration, vol. 288, pp. 387–394, 2005.

[13] R.W. Stark, G. Schitter, M. Stark and R. Guckenberger, “State space model of freely vibrating and surface-coupled cantilever dynamics in atomic force microscopy,” Phys. Rev. B, vol. 69, no. 8, 085412, 2004.

[14] Rafael Vazquez, F.-J. Rubio-Sierra and Robert W. Stark, Transfer Function Analysis of a Surface Coupled Atomic Force Microscope Cantilever System, Proceedings of the 2006 American Control Conference Minneapolis, Minnesota, USA, June 14-16, 2006

[15] F. Javier Rubio-Sierra, Rafael Vázquez, and Robert W. Stark, Transfer Function Analysis of the Micro Cantilever Used in Atomic Force Microscopy, IEEE TRANSACTIONS ON NANOTECHNOLOGY, VOL. 5, NO. 6, PP. 692-700, NOVEMBER 2006

[16] Jalili N, Dadfarnia M, Dawson DM. A fresh insight into the microcantilever–sample interaction problem in non-contact atomic force microscopy. ASME J Dyn Syst Measurements Control 2004; 126:135.

[17] Jalili N, Dadfarnia M, Dawson DM. Distributed-parameters base modeling and vibration analysis of micro-cantilevers used in atomic force microscopy. Proc 19th ASME Biennial Conf Mech Vib Noise, Symp Dyn Vibration Robotic Syst. Chicago, Illinois (September 2003).

[18] Ewan J. Barr, Modelling Atomic Force Micrscopy (Using An Euler-Bernoulli Beam Equation), Department of Engineering Mathematics, University of Bristol, March 2006.

[19] Kuo, Chung-Feng Jeffrey, Su, Te-Li, Li, Zheng-Lin and Chiu, Chin-Hsun (2007) 'Control System Design for Stability and Precise Positioning of Atomic Force Microscopy Probe', Polymer-Plastics Technology and Engineering, 46:9, 849 — 861.

[20] M.H. Mahdavi, A. Farshidianfar, M. Tahani, S. Mahdavi and H. Dalir, A more comprehensive modeling of atomic force microscope cantilever, Ultramicroscopy (2008), doi:10.1016/j.ultramic.2008.08.003

[21] Meirovitch, L. Dynamics and Control of Structures. John Wiley & Sons, Inc.: New York, 1990, 40–41.

[22] D. INMAN 1994 Engineering vibration. Englewood Cli!s, NJ: Prentice Hall, Inc.

[23] L. MEIROVITCH 1997 Principles and ¹echniques of <ibrations. Englewood Cli!s, NJ: Prentice Hall, Inc.

[24] S. S. RAO 1995 Mechanical vibrations, third edition. Reading, MA, Addison-Wesley Publishing Company.

Appendix I

The homogenous solution of Eq. (16) and its time derivatives can be expressed as:

$$\begin{aligned} W_h(x) &= C_1 \sin ax + C_2 \cos ax + C_3 \sinh ax + C_4 \cosh ax \\ W_h'(x) &= a\left(C_1 \cos ax - C_2 \sin ax + C_3 \cosh ax + C_4 \sinh ax\right) \\ W_h''(x) &= a^2\left(-C_1 \sin ax - C_2 \cos ax + C_3 \sinh ax + C_4 \cosh ax\right) \\ W_h'''(x) &= a^3\left(-C_1 \cos ax + C_2 \sin ax + C_3 \cosh ax + C_4 \sinh ax\right) \end{aligned} \tag{A1}$$

From boundary conditions we have:

$$W_h(0) = 0 \Rightarrow C_4 = -C_2 \tag{A2}$$

$$W_h'(0) = 0 \Rightarrow C_3 = -C_1 \tag{A3}$$

$$W_h''(L) = 0 \Rightarrow \left[\sin aL + inhaL\right]C_1 + \left[\cos aL + \cosh aL\right]C_2 = 0 \tag{A4}$$

And finally:

$$\begin{aligned} &-m_e\omega_n^2\left(D + \left[\sin aL - \sinh aL\right]C_1 + \left[\cos aL - \cosh aL\right]C_2\right) - a^3 EI\left(-\left[\cos aL + \cosh aL\right]C_1 + \left[\sin aL - \sinh aL\right]C_2\right) + \\ &k_{ts}\left(\left[\sin aL - \sinh aL\right]C_1 + \left[\cos aL - \cosh aL\right]C_2\right) = 0 \end{aligned} \tag{A5}$$

by defining B_1, B_2, B_3 and B_4 as:

$$\begin{aligned}
B_1 &= \sin aL + \sinh aL \\
B_2 &= \cos aL + \cosh aL \\
B_3 &= [\sin aL - \sinh aL][k_{ts} - m_e\omega_n^2] + a^3 EI[\cos aL + \cosh aL] \\
B_4 &= [\cos aL - \cosh aL][k_{ts} - m_e\omega_n^2] - a^3 EI[\sin aL - \sinh aL]
\end{aligned} \tag{A6}$$

Substituting (A6) in (A2-A5) gives:

$$\begin{aligned}
C_1 B_1 + C_2 B_2 &= 0 \\
C_1 B_3 + C_2 B_4 &= m_e \omega_n^2 D
\end{aligned} \tag{A7}$$

Therefore:

$$C_1 = \frac{B_2 m_e \omega_n^2 D}{B_2 B_3 - B_1 B_4} \tag{A8}$$

$$C_2 = -\frac{B_1 m_e \omega_n^2 D}{B_2 B_3 - B_1 B_4} \tag{A9}$$

$$C_3 = -\frac{B_2 m_e \omega_n^2 D}{B_2 B_3 - B_1 B_4} \tag{A10}$$

$$C_4 = \frac{B_1 m_e \omega_n^2 D}{B_2 B_3 - B_1 B_4} \tag{A11}$$

And the characteristic equation is expressed by:

$$B_2 B_3 - B_1 B_4 = 0 \tag{A12}$$